ACS APPLIED MATERIALS & INTERFACES

Research Article

www.acsami.org

Sonication-Assisted Layer-by-Layer Assembly for Low Solubility Drug Nanoformulation

Ana C. Santos,[†,‡] Pravin Pattekari,[§] Sandra Jesus,[†,‡] Francisco Veiga,[†,‡] Yuri Lvov,[§] and António J. Ribeiro*[,‡,∥]

[†]Center for Neuroscience and Cell Biology, University of Coimbra, Rua Larga, Faculty of Medicine, Pólo I, First Floor, 3000-504 Coimbra, Portugal

[‡]Faculty of Pharmacy, University of Coimbra, Azinhaga Sta. Comba, 3000-548 Coimbra, Portugal

[§]Institute for Micromanufacturing, Louisiana Tech University, P.O. Box 10137, Ruston 71272, Louisiana, United States

[∥]Institute For Innovation And Health Research, Group Genetics of Cognitive Dysfunction, Institute for Molecular and Cell Biology, Rua do Campo Alegre, 823, 4150-180 Porto, Portugal

Supporting Information

ABSTRACT: Sonication-assisted layer-by-layer (LbL) self-assembly is a nanoencapsulation technique based on the alternate adsorption of oppositely charged polyelectrolytes, enabling the encapsulation of low solubility drugs. In this work, a top-down LbL technique was performed using a washless approach and ibuprofen (IBF) as a model class II drug. For each saturated layer deposition, polyelectrolyte concentration was determined by titration curves. The first layer was constituted by cationic poly(allylamine hydrochloride) (PAH), given the IBF negative surface charge, followed by anionic polystyrenesulfonate (PSS). This polyelectrolyte sequence was made up with 2.5, 5.5, and 7.5 bilayer nanoshells. IBF nanoparticles (NPs) coated with 7.5 bilayers of PAH/PSS showed 127.5 ± 38.0 nm of particle size, a PDI of 0.24, and a high zeta potential (+32.7 ± 0.6 mV), allowing for a stable aqueous nanocolloid of the drug. IBF entrapment efficiency of 72.1 ± 5.8% was determined by HPLC quantification. In vitro MTT assay showed that LbL NPs were biocompatible. According to the number of coating layers, a controlled release of IBF from LbL NPs was achieved under simulated intestinal conditions (from 5 h up to 7 days). PAH/PSS-LbL NPs constitute a potential delivery system to improve biopharmaceutical parameters of water low solubility drugs.

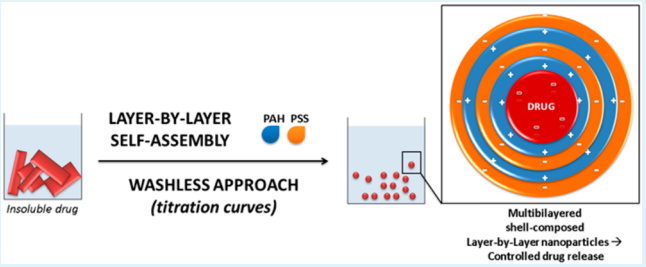

KEYWORDS: *layer-by-layer self-assembly, washless, colloid, electrostatic interactions, controlled release, oral delivery*

INTRODUCTION

The development of versatile and efficient nanoparticulate carriers for low solubility drugs is of outmost interest, due to the significant increase of the dissolution rate, which in turn can lead to increases in the drug bioavailability.[1]

Several nanoparticulate delivery systems have been recently developed; however, some limitations still have to be overcome. Micelles offer appropriate nanoparticle (NP) size, but for low water solubility drugs, low loading capacities are achieved.[2,3] On the other side, drug-loaded polymeric coacervates show larger particle sizes and low drug-loading capacities.[4] Synthetic polymer−drug conjugates have concerns related to lack of stability, low drug-holding capacity, and absence of controlled drug delivery.[5]

Layer-by-layer (LbL) self-assembly is a promising approach that assembles polyelectrolyte (PE) multilayer shells into drug-loaded particles.[6,7] LbL coating is obtained by the alternated addition of polycations and polyanions to the system under sonication, assembling thin PE shells on drug particles surface. After the first PE deposition, the highly charged polymeric layer is formed on the drug NP surface, preventing aggregation when the sonication stops.[8] Particles can display different properties based on the nature of the PEs and the architecture of the charged PE shell or the number of coating cycles.[9] These systems allow for high low solubility drug content and high aqueous physical stability.[10] The appropriate design of shell architecture at nanometer level enables the control of drug release.[8]

LbL fabricated PE particles have successfully modified the solubility of drugs; however, in most cases these systems showed a diameter of a few micrometers,[10] which is too large to increase drug dissolution velocity. Reducing particle size into the nanoscale leads to a surface area increase and, consequently, increases the drug dissolution velocity.[11] These formulation improvements together with the versatility of formed nanoparticulate carriers resulted in a growing interest in the

Received: March 5, 2015
Accepted: May 18, 2015
Published: May 18, 2015

DOI: 10.1021/acsami.5b02002
ACS Appl. Mater. Interfaces 2015, 7, 11972−11983

application of LbL drug delivery systems into the nanoscale.[12] Therefore, LbL NPs can be successfully employed if the dissolution velocity is the rate-limiting step for absorption of Biopharmaceutics Classification System (BSC) II drugs intended for the oral route.[13]

The production of LbL self-assembly NPs can be achieved using sonication by a top-down or a bottom-up approach. A top-down approach refers to a particle size reduction technique for drug direct nanoencapsulation. In this case, aqueous suspensions of micron sized drugs are submitted to sonication to decrease the size of drug to the nanoscale. The continuous sonication prevents fast agglomeration of smaller particles and the application of the LbL technology promotes suspension stabilization. On the other hand, the bottom-up approach is based on the drug nucleation in the cosolvent after its dissolution in organic solvent. Comparatively, the top-down approach has been shown to be more efficient in the preparation of large amounts of ∼200 nm capsules. The bottom-up approach, in turn, was shown to be more efficient in producing smaller capsules of ∼100 nm, but with lower product yield.[14] Moreover, the use of organic solvents used in bottom-up approaches raises environmental and human safety concerns over residual solvent. For these reasons, a top-down approach was chosen for this work.

The traditional LbL technique uses intermediate washings to remove the excess of PE after each layer deposition. These repetitive washings are time and PE consuming, conduct to process losses, and are less adaptable to common manufacturing processes.[8] New and detailed characterizations of LbL shell compositions produced without using intermediate washings are being reported to avoid these drawbacks. Using simultaneous sonication-assisted breakup of native microsized hydrophobic drugs into nanocrystals with PE adsorption yields coated nanocrystals in a process without intermediate centrifugations.[12] Thus, nanocoating layers formed in equilibrium or reduced PE concentrations are emerging toward the simplification and maximization of NPs production.[14,15]

Multiple works used 3−5 μm multilayer LbL shells to encase highly soluble proteins and drugs using sacrificial templates.[16−19] Nowadays, many efforts are directed toward encapsulation of low solubility drugs and perform drug direct encapsulation, avoiding the use of sacrificial cores.[10]

The design of LbL nanovehicle systems only recently reached the desirable level of properties for efficient systemic delivery such as minimum toxicity due to biodegradable materials, nanocolloidal stability using isotonic formulations, and prolonged in vitro and in vivo release of encased drugs.[12,20]

The LbL nanoencapsulation increased the solubility of curcumin,[21] tamoxifen,[8] paclitaxel,[8,14,15] resveratrol,[22] and camptothecin.[15,23] This technique has been successful by making use of either synthetic polymers such as poly(allylamine hydrochloride) (PAH),[14,22] polystyrenesulfonate (PSS),[14,22,23] and poly(diallyldimethylammonium chloride) (PDDA),[22] or natural polymers such as bovine serum albumin (BSA),[14,15,23] protamine sulfate,[14,22] chitosan,[14,22] alginate,[14,22] polyethylenimine,[15,23] poly-L-lysine,[15] and heparin.[23] The application of the LbL nanoencapsulation to increase the solubility of drugs to be administered orally requires a fully physicochemical characterization of the nanoparticulate system, a biopharmaceutical characterization through gastrointestinal (GI) simulating dissolution tests, biocompatibility, and biodegradability studies.

The novelty of the present work was to prepare low solubility drug-loaded NPs for oral delivery by sonication-assisted LbL top-down nanotechnology without intermediate washings. New architectured PE-coated shells were constructed. Ibuprofen (IBF) was chosen as a low solubility model drug, and PAH and PSS as PEs with low molecular weight, regarding their high surface charge, stability, and biocompatibility.[8] The resulting IBF NPs were characterized with regard to morphology, particle size, zeta potential, drug-loading, stability, in vitro release, and cytotoxicity.

EXPERIMENTAL SECTION

Materials. Poly(allylamine hydrochloride) (PAH, M_W ∼ 15 kDa), polystyrenesulfonate (PSS, M_W ∼ 75 kDa), fluorescein isothiocyanate (FITC), gel chromatography Sephadex PD10 columns (Amersham Biosciences, Wikströms, Sweden), 3-(4,5-dimethylthiazol-2-yl)-2,5-diphenyltetrazolium bromide (MTT) reagent, and Dulbecco's modified Eagle medium (DMEM) were purchased from Sigma-Aldrich (Steinheim, Germany). Fetal bovine serum (FBS) samples supplemented with PenStrep and trypsin were acquired from Life Technologies Corporation (Paisley, U.K.). IBF was kindly donated from Medinfar-Amadora, Portugal. Milli-Q water was used at pH 7.0−7.2. All other reagents were of analytical grade and were used as received.

Nanoparticles Preparation. IBF was dispersed at 0.5 mg/mL in 1−5 mL of Milli-Q water. For initial dispersion, IBF was sonicated 5 min using an ultrasound bath sonicator (Bandelin Sonorex Super, Bandelin, Berlin, Germany). IBF particle size and zeta potential were periodically measured during the sonication-assisted LbL procedure. Polycation PAH was used under continuous sonication to form the first surface layer, since IBF nanocores were found to bear intrinsic negative charge. To determine the PE concentration to completely coat IBF nanocore surfaces, PE titrations depending on zeta potential and particle size of NPs were made through the dropwise addition of PAH at 1 mg/mL to IBF NPs. After the first PAH layer addition, the LbL process was continued with the use of the titrated concentration of the oppositely charged PSS at 1 mg/mL. The LbL assembly was carried up to 7.5 bilayers of PAH/PSS shell, through the following alternate addition of PEs PAH and PSS. The formulations with 2.5, 5.5, and 7.5 LbL bilayers were considered for further studies which are discussed below.

Particle Size Analysis. The particle size and polydispersity index (PDI) were investigated by dynamic light scattering (DLS) using a particle size analyzer (DelsaNano C Submicron, Beckman Coulter Delsa, Krefeld, Germany). Mean diameter, size distribution, and PDI of aqueous NPs suspensions were determined for 5 min in triplicate at 25 °C with an angle measurement of 60°, after an equilibration time of 3 min. For each measurement, the NP suspension was diluted in Milli-Q water to an appropriate concentration to avoid multiple scattering. Results are presented as mean ± standard deviation, extracted from the Cumulants algorithm.[24,25] The instrument was checked and calibrated using standard latex nanoparticles (Beckman Coulter, Inc.).

Zeta Potential Analysis. Zeta potential measurements were taken by electrophoretic light scattering (ELS) using a Nano Zeta Potential Analyzer (DelsaNano C Submicron, Beckman Coulter Delsa, Krefeld, Germany). Measurements were taken in a Flow Cell (Beckman Coulter Delsa) at 25 °C, and Milli-Q water (pH 7.0−7.2) was used as diluent to proper concentration. The zeta potential was calculated using the Helmholtz−Smoluchowsky equation. Values are presented as means of triplicate runs per sample. The instrument was routinely checked and calibrated using a mobility standard (Beckman Coulter, Inc.).

Microscopic Analysis. An optical microscope equipped with a Digital Sight DS-U2 microscope camera controller was used to evaluate IBF crystals size and to check for IBF crystals presence in LbL NP formulations. The sample preparation was made by placing a 10 μL-drop of diluted NPs suspensions between glass slides.

The shape and surface morphology of NPs was monitored using a Jeol SM-6010LV/3010LA scanning electron microscope (SEM). For SEM analysis a 10 μL drop of diluted NPs suspension was placed onto

DOI: 10.1021/acsami.5b02002
ACS Appl. Mater. Interfaces 2015, 7, 11972−11983

Scheme 1. Schematic Presentation of LbL NP Formation from Low Solubility Drugs by Washless Top-Down LbL PE Assembly[a]

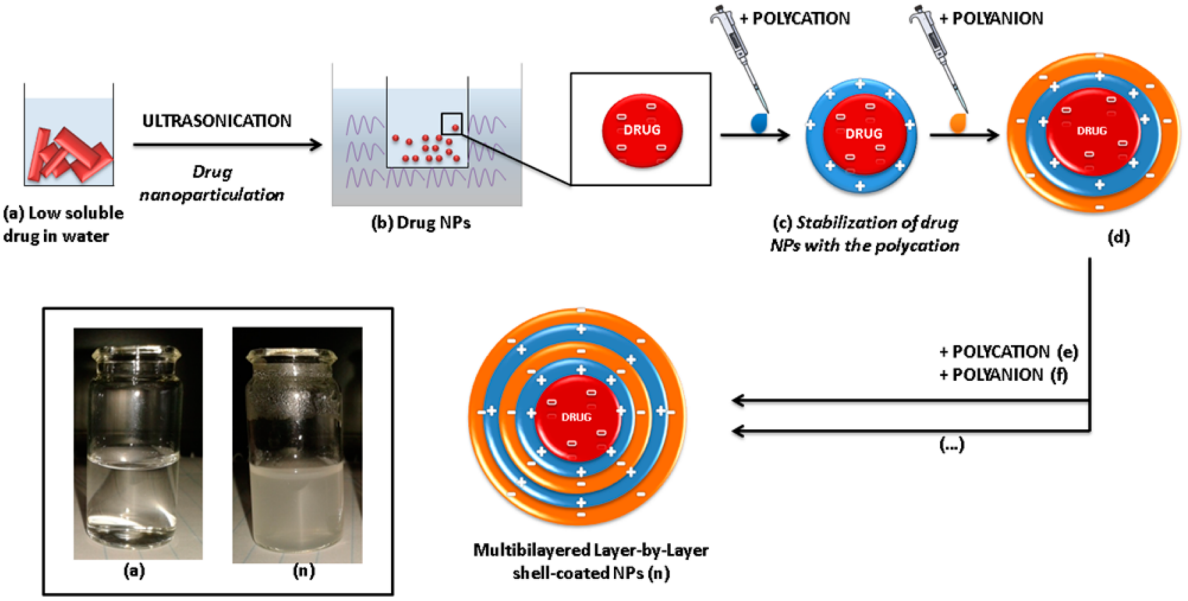

[a]Drug native microcrystals are first dispersed in water (a), and subjected to ultrasonication up to the attainment of drug NPs (b), followed by adsorption of a polycation layer (c) and polyanion layer (d) and so on (e, f, ...) up to the desired number (n) of PE bilayers upon the LbL shell, showing a characteristic naked eye Tyndal Effect (n).

a metal plate and kept overnight at room temperature inside a desiccator.

To control and confirm the deposition of polycation layers in the LbL shell formation, PAH was labeled with FITC, and NPs were monitored by using a laser scanning confocal microscope, Zeiss LSM 510 Meta (Carl Zeiss Inc., Göttingen, Germany), equipped with a 63× oil immersion objective Plan-ApoChromat with numerical aperture of 1.4. To obtain FITC labeled-NPs, PAH was tagged with FITC, based on a method described elsewhere.[26] FITC was covalently bound to PAH by the slow addition of FITC dissolved in dimethyl sulfoxide (DMSO) to the PAH buffered solution in excess, using a proportion of 0.05:1 (v/v). The FITC not utilized in the coupling reaction was removed by gel chromatography in a Sephadex PD10 column. The purified FITC-labeled PAH was stored in the dark at 4 °C until further use.

Determination of Drug Encapsulation Efficiency. Non-encapsulated IBF was separated from NP suspension by centrifugation (1000 rpm, 10 min) using an Eppendorf Mini Spin centrifuge (Hamburg, Germany). The IBF LbL NPs collected in the supernatant were analyzed for IBF, and the encapsulation efficiency (EE) of IBF is defined as the following equation (eq 1):

$$\text{encapsulation efficiency (\%)} = \frac{\text{actual amount of IBF loaded in NPs}}{\text{theoretical amount of IBF loaded in NPs}} \times 100 \quad (1)$$

For IBF quantification, IBF NPs were submitted to an extraction with the high performance liquid chromatography (HPLC) mobile phase 1:5 (v/v) followed by vortex agitation for 1 min and sonication for 5 min. IBF assay was performed with a HPLC column by using a previously HPLC reported method.[27] The HPLC analysis was carried out by a Shimadzu LC-2010CHT apparatus equipped with a quaternary pump, an autosampler unit, and a L2450 UV−vis dual wavelength detector. A RP18 (4.6 mm × 125 mm) Lichrospher 100 analytical column (Merck KGaA, Germany), with a precolumn, was employed for the analysis. The mobile phase consisted of a 60:40 (v/v) mixture of acetonitrile/water adjusted to pH 2.5 with orthophosphoric acid with a flow rate 1.0 mL/min, an injection volume of 20 μL, and detection at 264 nm at 30 °C.

Stability Studies. LbL NP formulation stability was evaluated by particle size and zeta potential measurements at specified time point over a total of a 14 days period. All measurements were carried out at room temperature (25 °C).

In Vitro Drug Release Assays at Sink Conditions. The release tests of IBF from NPs were performed in simulated gastric (pH 1.2) and intestinal (pH 6.8) fluids without enzymes, according to United States Pharmacopeia (USPXXIV).

In order to comply with sink conditions during in vitro release studies, the saturation solubility was determined. Excess IBF powder (60 mg) was added to 10 mL portions of both media, and these samples were kept under agitation for 24 h (37 °C/100 rpm). Aliquots of 2 mL each were withdrawn every 2 h and immediately centrifuged (13 400 rpm/10 min). The supernatant was filtered using a 0.45 μm syringe filter (GHP Acrodisc, Pall Gelman Laboratory), and the filtered samples after suitable dilution were assayed for IBF by HPLC, as described above. All syringes, pipettes, filters, and vials used were preheated to 37 °C in an oven. The solubility experiments were performed in triplicate (n = 3).

For the release studies, 1.5 mL of purified IBF-loaded NPs suspension was sealed into a dialysis membrane bag[28] with a molecular weight cutoff of 3500 Da. The membrane was immersed into 50 mL of each media at 37 °C and stirred at 100 rpm. At fixed intervals, 0.5 mL of medium was withdrawn and filtered using a 0.45 μm syringe filter. At the same time, the same volume of fresh medium was added to the release medium. The concentration of released IBF was determined by HPLC, using the previously described method. In vitro IBF release studies were performed in triplicate (n = 3).

Cytotoxicity MTT Assay. The cytotoxicity of LbL NPs against Caco-2 cells was studied using an MTT assay. Caco-2 cells were obtained from European Collection of Cell Cultures and were used after 71−74 passages. The cells were cultured at 37 °C and 5% CO_2, in DMEM with 10% FBS supplemented with 1% PenStrep. Subcultures were performed by detaching the cells with trypsin. These studies were performed after 18 h incubation of 100 μL of a Caco-2 cell suspension

DOI: 10.1021/acsami.5b02002
ACS Appl. Mater. Interfaces 2015, 7, 11972−11983

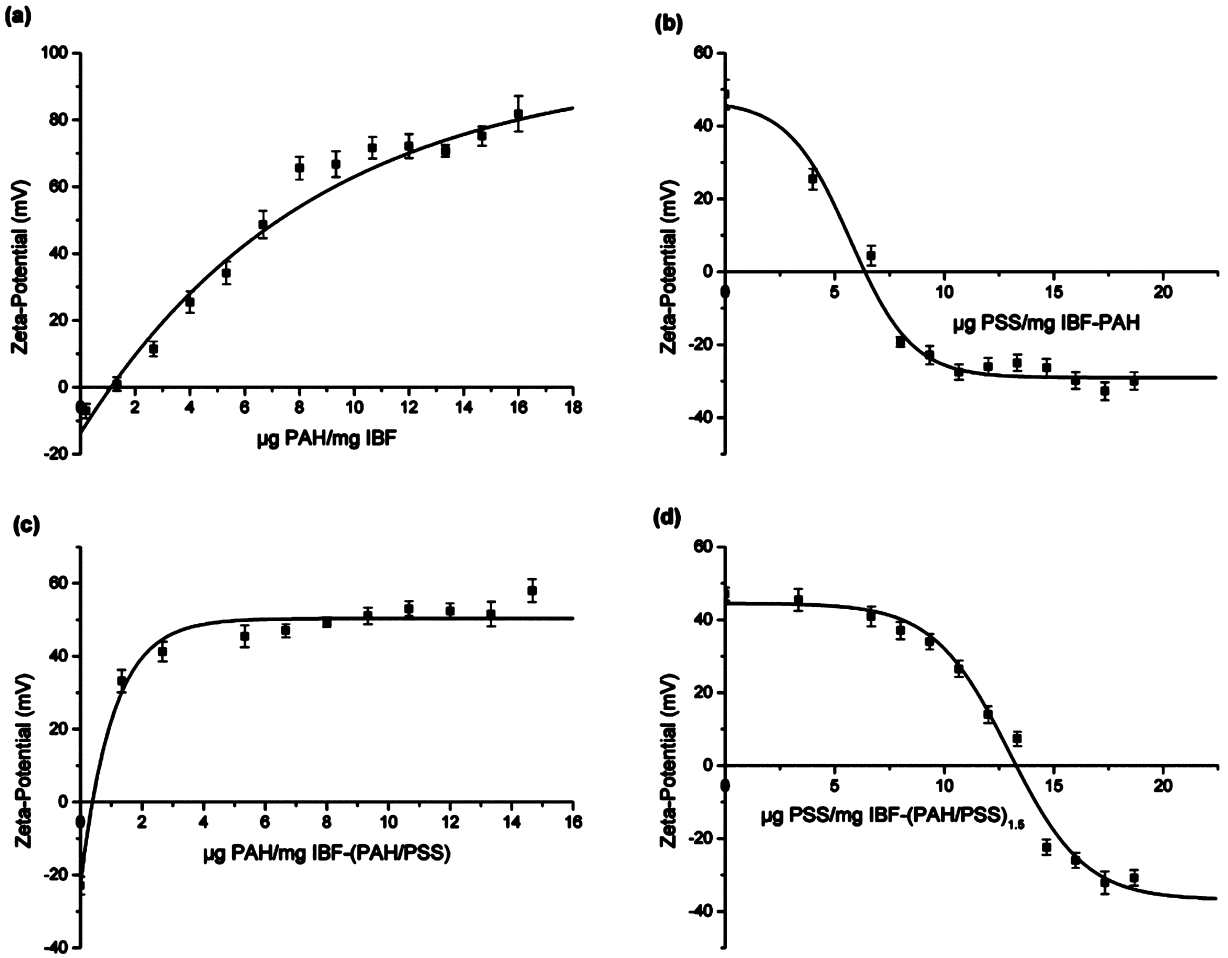

Figure 1. Zeta potential against PE concentration for 0.5 mg/mL IBF NPs. Four sequential steps of polycation/polyanion deposition are shown in the stepwise addition of (a) PAH to IBF nanocores, (b) PSS to IBF-PAH NPs, (c) PAH to IBF-(PAH/PSS) NPs, and (d) PSS to IBF-(PAH/PSS)$_{1.5}$ NPs.

seeded in a 96-well plate at a density of 10^5 cells/mL. Prior to the addition of the NPs, the medium was removed, and 100 μL of new complete medium was added. Serial dilutions of the LbL NPs were prepared in DMEM free of serum at a concentration range between 11.7 μg/mL and 1500 μg/mL. 100 μL of each NPs sample were added and incubated with the cells for 24 h, at 37 °C and 5% CO_2. After 24 h, the MTT cytotoxicity assay was performed. The cell viability (%) related to control (cells in culture medium without NPs) was calculated by the following equation (eq 2):

$$\text{cell viability (\%)} = \frac{\text{ODsample(540 nm)} - \text{ODsample(630 nm)}}{\text{ODcontrol(540 nm)} - \text{ODcontrol(630 nm)}} \times 100 \quad (2)$$

RESULTS AND DISCUSSION

The sonication process was shown to be able to reduce IBF native micron ranged crystals (Scheme 1a) to the nanometer scale (Scheme 1b). Keeping these IBF NPs under sonication prevented their fast agglomeration. Subsequently, the application of LbL coating, by the adsorption of successive alternating charged PE coatings of PAH and PSS, allowed for colloidal stabilization (Scheme 1c–n). Sufficient PE concentrations for each shell layer saturated deposition were determined by tracing titration curves (Figure 1), avoiding unwanted intermediate washings. A top-down approach using a washless LbL technique produced successfully PAH/PSS-constituted multilayer shell NPs containing IBF. These NPs are proposed as potential oral delivery systems for a low solubility drug. NP process formulation and characterization are described below in detail.

Layer-by-Layer Preparation and Characterization of Ibuprofen Nanoparticles. *Titrations of Polyelectrolyte Concentrations.* Initially, the intrinsic magnitude charge of IBF nanocores was determined by a zeta potential measurement. A value of −15.1 ± 2.1 mV reflected the IBF nanocore's negative surface charge, as shown in the first point of the titration in Figure 1a. Since the LbL process is based upon electrostatic interactions between the core drug and the PEs, the surface charge determination of the core drug was crucial to knowing the order of addition of the PAH/PSS PE pair to cover its surface. In this study, the first added PE was the PAH polycation, followed by the addition of PSS polyanion second.

In order to establish an optimal sonication-time condition, the sonication time required to achieve the first PE coating layer (which corresponded to the IBF nanocores' surface coating with PAH) was tested for particle size. As can be seen in Figure 2, sonication time strongly influenced particle size, and a 20 min sonication of initially low solubility IBF microcrystals in the presence of PAH allowed the attainment of IBF-PAH NPs with a particle size of 122.0 ± 37.6 nm and a PDI of 0.24. NPs formation was confirmed by suspension opalescence associated with the Tyndall effect as depicted in

DOI: 10.1021/acsami.5b02002
ACS Appl. Mater. Interfaces 2015, 7, 11972–11983

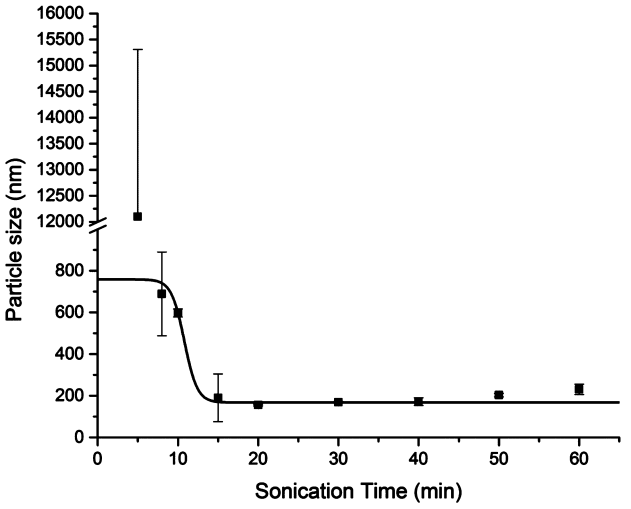

Figure 2. Particle size of IBF cores, with ~73 μm of initial particle size, in response to sonication time. PAH was present in solution for the first polymeric monolayer on the IBF nanocores surface and prevented particle aggregation after the removal of ultrasound.

Scheme 1n. Further increase in the sonication time beyond 20 min did not decrease particle size, and after 40 min the particle size started to slightly enhance. This was probably a consequence of the bridging of larger drug particles with the PE.[14] After the coating layer deposition of PAH over IBF nanocores, the strongly positive charge prevented aggregation and maintained colloidal stability to continue LbL shell formation with more coating PE layers.

After optimization of the sonication time, the ideal PE concentration for each coating layer was examined. Regarding this, a range of PE concentrations were investigated for each layer, and the resulting zeta potentials were measured. The stepwise PE addition enabled the construction of the respective titration graphs, depicted in Figure 1. In practice, this corresponds to the complete PE deposition on the NPs surface for each LbL coating layer, determined by the recharging point in each titration curve. This point was the requisite to proceed for the next PE coating layer deposition.

Starting with IBF nanocores, the titration curve regarding the PAH surface deposition is depicted in Figure 1a. As can be seen, the point of plateau for the zeta potential started at 6.7 ± 4.1 μg PAH/mg IBF. After PAH addition and complete surface coating, the PE was switched to negative polyanion PSS, and that titration corresponds to Figure 1b. The titration of IBF-PAH NPs enabled the determination of the point of the plateau at 9.3 ± 2.5 μg PSS/mg IBF. In the third step, PAH was added to IBF-(PAH/PSS) NPs, and the point of plateau was 6.7 ± 1.8 μg PAH/mg IBF, as shown in Figure 1c. The fourth titration graph, Figure 1d, shows the addition of PSS to IBF-(PAH/PSS)$_{1.5}$ NPs, and the corresponding value was 14.7 ± 2.1 μg PSS/mg IBF. Thus, it is noteworthy that the addition of the following coating PE layer was only performed after adding the previously determined ideal concentration.

The analysis of the titration curves of IBF nanocores when using cationic PAH and anionic PSS enabled the observation of differences. Upon PAH addition, an increasing effect on zeta potential value along with a more gradual plateau onset were verified, following an exponential fitting model (R^2 > 0.97 for both titrations, Figure 1a,c). On the other hand, PSS originated a clear plateau onset point, approaching a sigmoid fitting model (R^2 > 0.95 for both titrations, Figure 1b,d). This difference could be explained by the difference in charge density of the used PEs. PAH shows more molecular loops and tails than PSS,[29] and it was only partially charged at the pH assay (neutral, pH = 7.0), giving the origin of thicker layers that can have hidden negatively charged patches. Furthermore, when PAH constituted the outermost layer, the highly positively charged molecules adhered to the previous layers and also protruded into the dispersion medium. This phenomenon increased PAH density and charge, which directly influenced zeta potential but in parallel created a lack of complete PE saturation, as is visible in the titration curves of Figure 1a,c. On the other hand, the addition of PSS to positive surfaces had just a little influence on the surface charge values, initially. This was due to the adsorption of PSS in the interior PAH loops. After overcoming PAH tails and loops, PE molecules started to form negative patches on the surface until achieving complete surface coverage, when a steep change in zeta potential values occurred, contrary to the PAH behavior.[29] This fact is related to the washless LbL technique which allows the achievement of thinner PE coating layers, more encompassed layers, and thus more PEs chains interpenetration.[30]

As it can be seen in Figure 1, titrations were only depicted for the first four PE coatings, as previously discussed. However, titrations were performed and analyzed up to two and a half PEs bilayer, namely, IBF-(PAH/PSS)$_{2.5}$. The two and a half PE bilayer formulation (IBF-(PAH/PSS)$_{2.5}$) was the less complex studied formulation. For this reason, it was considered for physical stability evaluation before addition of further LbL coatings, and consequently before the preparation of more complex formulations. These NPs were shown to be physically stable for at least 1 week, as is depicted in Figure 3a. Once physical stability with two and a half bilayers was acquired, the complete titration procedure for each next coating step, which was shown to be a tedious and slow protocol, was therefore avoided. The addition of the PE layers after the two and half PE bilayers was done just until sufficient physical stability was obtained. This was attained without precisely determining the critical plateau point as before, namely, by the determination of the PE concentration that allowed for charge reversal without aggregation. In practice, it corresponded to the attainment of +20 and −15 mV zeta potential magnitudes without significant changes in particle size for PAH and PSS coatings.

After all the LbL coatings were done through the determination of necessary PE concentrations for each PE layer coating, IBF LbL-coated NPs were produced by ensuring no PE excess for the LbL successive coatings. A washless technique was developed for PAH/PSS coating up to 7.5 bilayers with homogeneous particle size populations at the desired nanoscale interval (100−200 nm).

Three different formulations of IBF NPs were studied, namely, with 2.5, 5.5, and 7.5 PE LbL bilayers.

Zeta Potential. The values of zeta potential magnitudes monitored during the process of sequential PAH/PSS adsorption upon IBF nanocores are present in Figure 4. The results showed that after adsorption of PAH to IBF nanocores with negative surface under sonication, drug NPs were recharged to a high positive surface charge (+60.0 ± 4.1 mV). These values revealed that the first PAH layer conferred high physical stability to the IBF nanocores. LbL assembly proceeded with the addition of the polyanion PSS, and the surface charge was again reversed to negative values (−22.8 ± 2.5 mV). The addition of the PAH constituted-third shell layer

DOI: 10.1021/acsami.5b02002
ACS Appl. Mater. Interfaces 2015, 7, 11972−11983

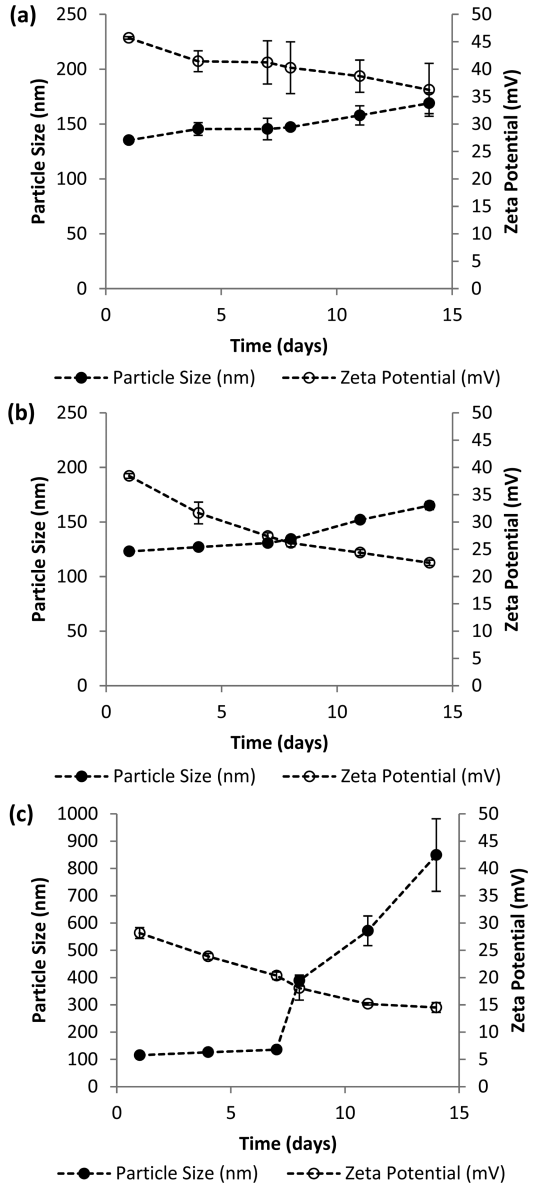

Figure 3. (●) Particle size and (○) zeta potential changes of IBF LbL NPs prepared with (a) 2.5, (b) 5.5, and (c) 7.5 bilayered coatings of PAH/PSS IBF for 14 days at 25 °C.

(one and half PEs coating bilayer) again promoted charge reversal, by the formation of a highly positively charged layer. The LbL assembly was proceeded by consecutively alternating both PE additions. The most complex performed formulation corresponded to the IBF NPs coated with a multilayer shell of 7.5 PAH/PSS bilayers, showing zeta potential higher than +30 mV.

As shown in Figure 4, the high surface potential remained constant during all the studied PE layer depositions up to the 2.5−3.0 bilayers. After this point a slight reduction on the magnitude of zeta potential was observed, depicted in the shrinkage of the final part of graph. Furthermore, the values showed significant differences between initial and final LbL shell coatings, corresponding to zeta potential values either for PAH and PSS layers. This happened due to the partial PE coating of the outermost layers, as well as due to the existence of secondary interactions between PEs of different bilayers, which triggered a decrease in the surface charge density.[31] Given the higher zeta potential magnitude of PAH layers (around +40 mV) compared to PSS layers (close to −20 mV), PAH was the chosen PE for the last layer, providing higher stability to these formulations.

The evaluation of zeta potential values during LbL assembly demonstrated alternation of the surface potential due to sequential polycation/polyanion deposition steps, confirming the surface recharging, the driving force of the process. This recharging, in turn, led to the conclusion that PE attachment to the NPs surface occurred and the complete coating was formed after each PE deposition step.

Particle Size. Particle size of NPs was evaluated after each layer deposition during the LbL assembly technique, and the results are depicted in Figure 5.

LbL technique allowed for homogeneous size distributions of 100−150 nm with PDI values around 0.20 for all LbL formulations. This suggested that NPs had an acceptable monodispersity distribution, without aggregation. Focusing on Figure 5, it is possible to see that during LbL assembly particle size suffered oscillation, which depended on the PE nature of the outermost layer. Particle size was significantly higher than 200 nm when PSS was used as the outermost coating layer of the LbL shell. The difference in the particle size, together with the previously discussed corresponding zeta potential analysis, suggested a slight aggregation process when using PSS. This behavior was reversible by the addition of the next PAH layer.

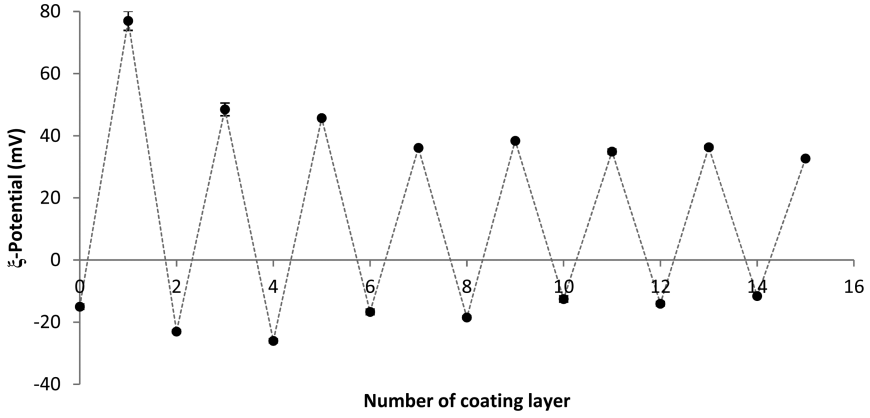

Figure 4. Zeta potential changes of IBF coated up to 7.5 coating bilayers, IBF-$(PAH/PSS)_{7.5}$, during process shell assembly, by top-down and washless approach.

DOI: 10.1021/acsami.5b02002
ACS Appl. Mater. Interfaces 2015, 7, 11972−11983

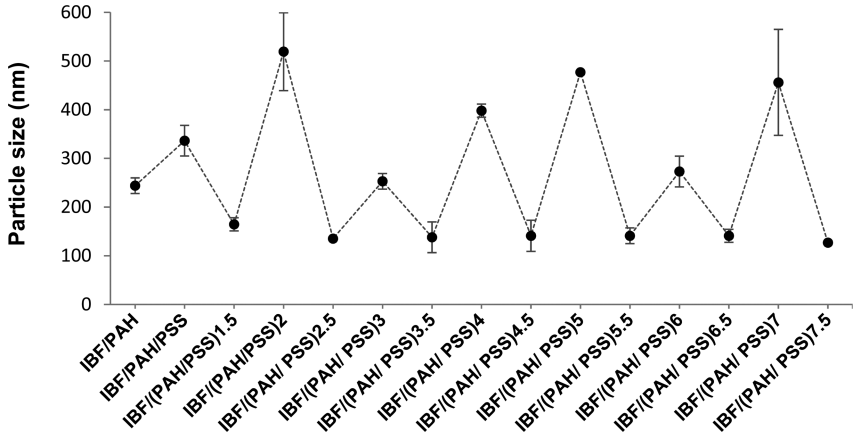

Figure 5. Particle size measurements of IBF coated up to 7.5 coating bilayers, IBF-$(PAH/PSS)_{7.5}$, during process shell assembly, by top-down and washless approach.

Table 1. Particle Size, Zeta Potential, and Encapsulation Efficiency of Ibuprofen Crystals and Ibuprofen Layer-by-Layer-Coated Nanoparticles

formulation	particle size (nm)	PDI	zeta potential (mV)	EE (%)
nonencapsulated IBF native crystals	73 000 ± 46 000	NA[a]	−15.1 ± 2.1	NA[a]
IBF-$(PAH/PSS)_{2.5}$ NPs	135.3 ± 1.9	0.20	+45.7 ± 0.2	78.1 ± 3.9
IBF-$(PAH/PSS)_{5.5}$ NPs	141.1 ± 16.0	0.20	+34.9 ± 0.8	74.4 ± 4.3
IBF-$(PAH/PSS)_{7.5}$ NPs	127.5 ± 38.0	0.24	+32.7 ± 0.6	72.1 ± 5.8

[a]NA = not applicable.

Observed NPs restabilization was caused by the phenomenon of NPs collapse in the presence of oppositely charged PEs able of decrease their interparticle bridging activity. Also, this occurred due to the increased particle surface charge, which led to higher electrostatic repulsion and decrease of the area occupied by single polymer molecules. In fact, when using PSS as the outermost coating layer in the LbL coating shell, zeta potential values were dominated by the anionic PE charge. However, the surface was still patched with protruding positive PAH chains which could have attached to negatively charged regions of other particles and have caused higher aggregation.[29] Thus, as PAH conferred higher physical stability to the NPs, this PE was used at the outermost layer of the LbL shell architecture in all of the three present studied NPs formulations.

Nanoparticle Imaging. The morphology and particle size of IBF NPs samples formulated by the LbL technology into the nanocolloidal state were evaluated by SEM and confocal microscopy. Supporting Information Figure S1 shows SEM images of native IBF crystals (Figure S1a) and prepared IBF LbL NPs (Supporting Information Figure S1b).

These images showed the reduction of characteristic needle-like shaped original IBF microsized crystals (73 ± 46 μm) to the nanoscale (100−150 nm), by the formation of square-like shaped NPs. Probably, this shape of NPs reflected IBF crystalline structures after LbL coating under sonication.[22]

It can be seen also that particle size analysis by SEM results (even without a high resolution) are in agreement with the sub-micron-sized colloidal particles obtained by DLS, depicted in Figure 5 and Table 1.

FITC-labeled PAH was prepared in order to formulate fluorescent LbL NPs (Supporting Information Figure S1c). Although the resolution of the confocal microscope (close to 100 nm) did not allow for detailed structure visualization, it was possible to see well-dispersed fluorescent green dots, which color is due to FITC labeling. This fluorescence of NPs confirmed the attachment of the fluorescent PAH to the NPs LbL shell. In order to overcome the confocal microscopy resolution limit and better confirm the presence of the PAH PE layer upon IBF nanocores surface, larger particles (microparticles) were prepared. These NPs were achieved using a shorter sonication time (5 min) with just one PAH-labeled FITC layer adsorbed on surface cores of IBF (Supporting Information Figure S1d). It can be seen that there is a micrometer-sized LbL capsule cross-section which provides evidence for the capsule wall, and therefore there is evidence of the successful adsorption of PEs during the LbL technique.

Encapsulation Efficiency. Encapsulation efficiency of the drug is an important index for drug delivery systems. The number of coating layers did not affect the encapsulation efficiency of IBF, which was higher than 70% for all the studied formulations (Table 1). It can be concluded that IBF was attached to PAH with high efficiency in the first step of LbL coatings. As the encapsulation process was conducted by electrostatic interactions, the first used PE in the LbL shell was PAH that has many amine groups,[32] which bound negatively charged IBF in pH 7.0. The main loss was due to the process, namely, the occurrence of splashed out particles of the container under powerful sonication during the LbL process. The present LbL NPs allowed the solubilization of IBF in water, and therefore, this delivery system can be applied for encapsulation of other II class drugs.

Stability Studies. One of the major aims of a nanoformulation is to maintain the colloidal stability in order to preserve its inherent physicochemical properties. Stability studies of the LbL-coated NPs with 2.5, 5.5, and 7.5 PE bilayers were performed over 14 days at room temperature (Figure 3). In these conditions, particle size was not affected during the first 7 days for all the formulations. After 7 days, all formulations showed a particle size enhancement, which could

DOI: 10.1021/acsami.5b02002
ACS Appl. Mater. Interfaces 2015, 7, 11972−11983

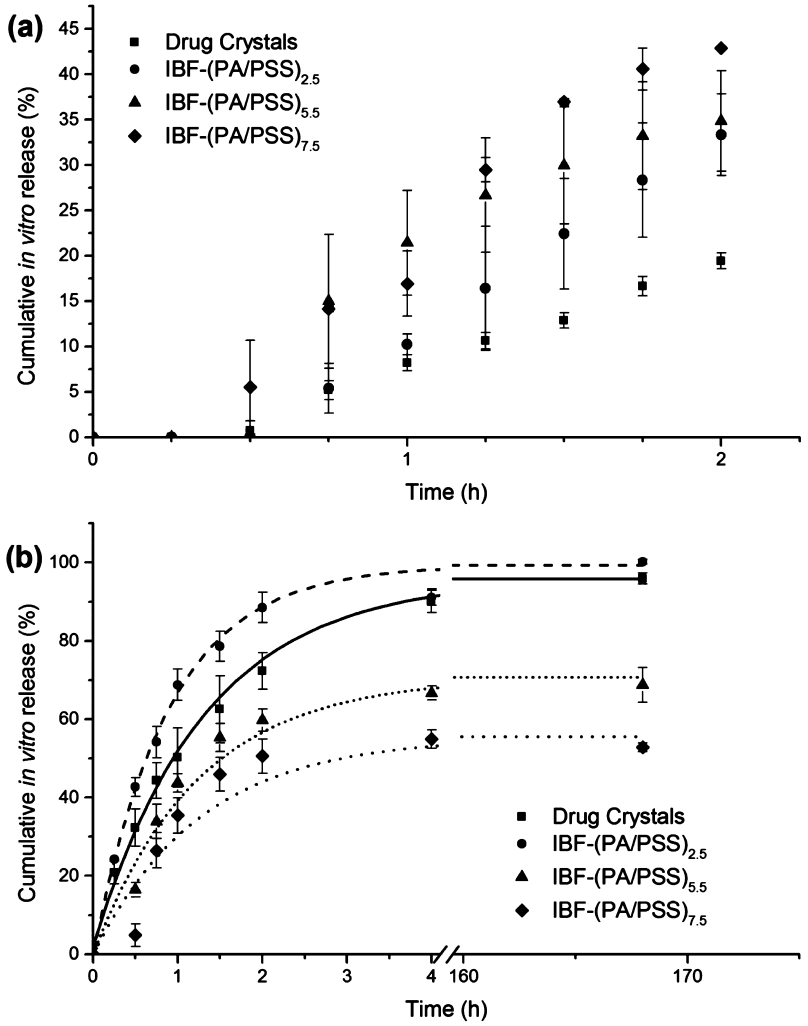

Figure 6. In vitro IBF release from (■) nonencapsulated crystals of IBF, and IBF LbL NPs prepared with (●) 2.5, (▲) 5.5, and (◆) 7.5 bilayered coatings of PAH/PSS in (a) simulated gastric pH 1.2 fluid and (b) simulated intestinal pH 6.8 fluid in sink conditions at 37 °C. Data represent mean ± SD, n = 3.

be caused by a zeta potential decrease, that could lead to aggregation phenomena. This effect was more pronounced for the most complex formulation (7.5 bilayers), whose particle size values were significantly different in relation to the other two formulations (2.5 and 5.5 bilayers). This was probably due to the enhancement of the LbL shell complexity, which triggered the existence of more bridging interactions between neighboring particles. For 5.5 and 7.5 bilayered formulations, changes were slighter in particle size and zeta potential during the same period. Given these results, it was possible to conclude that aqueous LbL-coated NPs were stable for 7 days at room temperature. However, after this period of time, stability was significantly decreased when the complexity of the shell was enhanced. These results were in accordance with heparin/PLB16-5-coated LbL NPs, that had shown higher particle size values when the shell was composed with 7 bilayers compared to 5 bilayers after 7 days at room temperature.[23]

In Vitro Release Studies. As IBF is a weakly acidic drug, the release from LbL NPs may be pH-dependent. In order to assess the potential of the LbL NPs to be used in drug delivery systems, release studies of IBF native crystals (nonencapsulated IBF) and IBF LbL NPs with different numbers of layered PAH/PSS shells were carried out in simulated gastric and intestinal fluids without enzymes at pH 1.2 (Figure 6a) and 6.8 (Figure 6b), respectively, maintaining body sink conditions.

As can be seen in Figure 6a, IBF native crystals showed a lower dissolution profile in simulated gastric fluid in relation to studied formulations of LbL NPs due to larger sized crystals in relation to the NPs size,[15,33] concomitantly with the low IBF solubility in this medium.[34] On the other hand, no effect on dissolution rate of encapsulated IBF was observed among the studied formulations of LbL NPs. Thus, no effect of shell wall thickness on IBF dissolution was detected. Drug release was overall faster for encapsulated IBF in relation to IBF native crystals, and no correlation of IBF release with a release kinetics model was found to be satisfactory in this release medium. Regarding studied formulations of LbL NPs, at simulated gastric pH the PAH/PSS capsule membrane was destabilized due to the pK_a of the PEs, affecting its integrity, and membrane permeability was increased due to the pore formation,[35] allowing for drug release. However, it is noteworthy that after 2 h of in vitro simulated gastric incubation, most IBF remained associated with LbL NPs (around 60%).

In simulated intestinal fluid (Figure 6b), it can be observed that LbL NPs allowed for a biphasic drug release pattern, with an initial burst release followed by a controlled drug release

DOI: 10.1021/acsami.5b02002
ACS Appl. Mater. Interfaces 2015, 7, 11972−11983

phase, showing a very good fit (R^2 > 0.99 for all formulations) with the exponential kinetic model following an apparent first-order behavior. The release pattern of these NPs initially revealed high release rate of IBF in the first 1.5 h, which can be attributed to the diffusion of some adsorbed IBF molecules onto the NPs' external surface. It was followed by a controlled IBF release phase attaining a plateau at 4 h in release medium without significant changes in the IBF release up to 170 h (7 days). In a comparison of the different LbL studied formulations, in 2 h, only 50.6% of IBF in 7.5-bilayered LbL NPs was released as compared with of 59.7% of the 5.5-bilayered LbL NPs, and 88.5% of the 2.5-bilayered NPs. An increasing effect of the number of coating bilayers on delayed release of IBF was observed. This effect was probably due to the enhancement of shell wall thickness of NPs, which increased the diffusional path for the encapsulated IBF and, thus, was conducted for an IBF diffusion delay from the core to the LbL net-like structure of oppositely charged PE-composed shell.[36] These factors resulted in a decrease of the IBF release rate and also in a decrease of the initial IBF burst release. Similar results were found using other low water-soluble drugs, like paclitaxel and isoxyl from nanocapsules.[14,33] Like in the present LbL NPs, the dissolution rate was found to decrease almost linearly with increasing shell thickness. In fact, a prolongation of drug release through the use of three coating PE bilayers was stated to be already effective.[33] Thus, an effect of LbL shell thickness on the dissolution enhancement was found also for those low solubility drugs. In another case, under sink conditions in PBS buffer pH 7.2, 40% of paclitaxel was released from $(PAH/BSA)_3$-coated NPs in 8 h as compared with 80% for one layer coated NPs.[14] It must be emphasized that IBF delayed release from LbL NPs was much higher when compared to IBF release from chitosan/dextran sulfate LbL microcapsules with 30 PE layers.[16] In 2 h at pH 1.4, previous microcapsules released close to 100% of the IBF while in the present NPs less than 40% of IBF was released at similar conditions. In higher pH the difference was even higher, whereas microcapsules released all the encapsulated IBF in less than 1 min at pH 7.4 compared to 4 h of delayed release from NPs at similar conditions (pH 6.8). Theoretically, when comparing LbL systems with similar PEs coating shells compositions, lower-sized particles could lead *higher* dissolution rate and thus higher drug release.[12] However, other factors are present in LbL formulations which influence drug release pattern besides particle size, and a higher capacity of drug delayed release in LbL NPs was verified when compared to LbL microcapsules. As pore radius decreases with decreasing particle size,[37] the lower pore size distribution of the nanopores of the NPs' LbL shell and their pore−matrix structure probably allowed for a lower displacement of the drug through the pores, decreasing PE shell permeability,[38] and thus delaying drug release in relation to micropores present in microcapsules. The nature of the PEs could also have contributed to this behavior, since synthetic PEs show more resistance to environmental changes than the natural PEs.[39]

The previously described increase in the LbL film thickness effect was also responsible for incomplete IBF release from the 5.5 and 7.5 PE bilayered formulations. Nonreleased IBF was confirmed to be inside LbL NPs through IBF quantification inside in vitro release dialysis membranes, which was shown to be in accordance to the maximum IBF released percentage (the asymptotic value of the release model fitting), namely, ∼30% and ∼50% of nonreleased IBF for 5.5 and 7.5 LbL bilayers. The high electrostatic-based linkage of the PEs web around the drug core seemed to enhance the strength with the number of LbL PE bilayers. With the increase of the complexity of the LbL shell, a lower fraction of free IBF was capable of diffusing to the exterior. In addition, the nondegradable nature of the used PEs can also have contributed to this behavior. Noncomplete drug release from LbL PE bilayered shells was also exhibited for higher layers number-composed LbL shells in previously reported release profiles.[14,15]

2.5-Bilayered LbL NPs, which corresponded to the less complex LbL formulation, led to IBF's slightly faster release in relation to nonencapsulated IBF. This was caused by the NP's smaller size and higher surface area in the formulation compared to micrometer size and lower surface area of the nonencapsulated IBF crystals. According to the Kelvin equation, the increase in the curvature of the particle surface triggers the increase in the dissolution pressure of the substance, with solubility being substantially increased as particle size decreases up to the nanoscale.[40] The increased solubility (or saturation solubility) of the drug is correlated to a faster dissolution rate by the Noyes−Whitney equation.[11] These results were in accordance to PLB16-5/Hep bilayered LbL NPs which did not show significant influences on the drug release rate for LbL shells thinner than 3.5 bilayers.[15]

PAH/PSS composed-shell LbL NPs showed a pH-dependent drug release behavior, as previously reported.[19] A suitable gastro-resistant approach should be used to avoid drug release in acidic medium, like gelatinous gastro-resistant capsules or the use of an enteric coating polymer with a molecular weight lower than 65 kDa to prevent colloidal aggregation.[41]

Cytotoxicity Assays. In vitro cytotoxicity evaluation can be performed to screen pharmaceutical formulations before testing in animals.[42] MTT assay was chosen because is one of the well-established cell viability assays, which is based on the capacity of the cellular mitochondrial dehydrogenase enzyme in living cells to reduce the yellow water-soluble MTT into a purple formazan,[43] therefore not evaluating the cell but its mitochondrial activity.[44] Caco-2 cells were used considering the intended oral route of the NPs.

Previous studies had shown a good cytotoxic profile for PAH/PSS capsules on different cell lines, which depended on the dosage and also on the capsule's size.[45,46] The outermost membrane layer effect on the toxicity had also been reported before on L929 cell line, and results indicated comparable results for PAH and PSS.[47] In this work, the choice of PAH as the outermost layer was previously explained with formulation aspects. The potential cytotoxicity of PAH/PSS-constituted LbL IBF NPs was evaluated with different numbers of coating bilayers (2.5, 5.5, and 7.5 bilayers) by determining the viability of the Caco-2 cells when exposed to NPs formulations (Figure 7).

A very good cytotoxicity profile was observed, indicating an in vitro cytocompatibility of the LbL NPs in this cell culture system. The concentrations where the cell viability decreased to 50% (IC_{50}) were 845.1 ± 1.1, 771.2 ± 1.1, and 698.9 ± 1.1 μg/mL for 2.5, 5.5, and 7.5-bilayered NPs, respectively. In the presence of higher concentrations, the three mentioned NPs formulations promoted a considerable increase in cytotoxicity, wherein almost no cell viability was achieved at 1500 μg/mL. This concentration-dependent toxicity can be caused by the instability obtained with higher NPs concentrations. Higher concentrations led to agglomeration on the cell culture medium and consequently sedimentation over the adherent cells causing their death. For lower concentrations, the electrostatically

DOI: 10.1021/acsami.5b02002
ACS Appl. Mater. Interfaces 2015, 7, 11972−11983

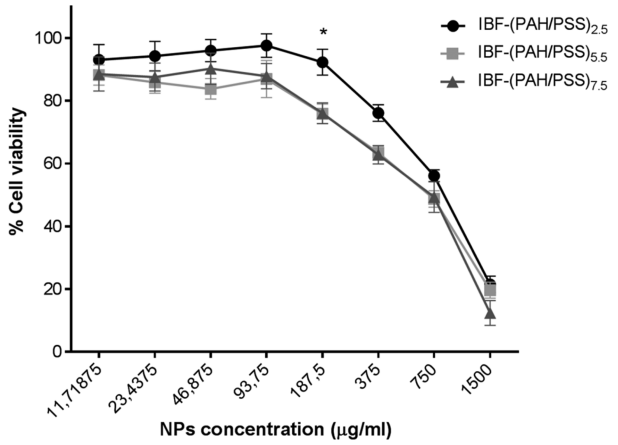

Figure 7. Cell viability of Caco-2 cells after 24 h of incubation with (●) 2.5, (light gray ■) 5.5, and (dark gray ▲) 7.5 LbL bilayer coated PAH/PSS NPs for concentrations ranging from 11.7 to 1500 μg/mL. Cell viability of each sample was determined using an MTT assay. Data are expressed as mean ± SEM (n = 14). *p < 0.05 for the 2.5 bilayered NPs in comparison to 5.5 and 7.5 bilayered LbL NPs.

induced repulsive bilayered LbL coatings of the NPs were probably responsible for NPs suspensions stability in the in vitro testing conditions, favoring NPs−cell interactions.[48] Beyond this, in a comparison of the cytotoxicity between the three different NPs formulations, it was possible to see that no statistical differences were observed along tested concentrations excluding the 187.5 μg/mL, where the 2.5 bilayered-coated LbL NPs showed statistically significant higher cell viability compared to the other two formulations. In consideration of the zeta potential values for the 3 systems, this result could be attributed to the more cationic profile of the 2.5-bilayered NPs that leads to a stronger interaction with the negatively charged cell membrane.[49] The positive surface charge of PAH/PSS LbL shells may have caused cell membrane pore formation followed by cell damage and death.[50] Nevertheless, considering the range of the whole experiment, these results demonstrated that the present LbL NPs system has a large range of no toxic in vitro concentrations, constituting a promising nanocarrier for low solubility drugs and enabling further in vitro/in vivo applications.

CONCLUSIONS

A sonication-assisted top-down approach along with a washless LbL technique was applied for nanoencapsulation of poorly water-soluble drug IBF by using a PAH/PSS-constituted shell up to 7.5 bilayers NPs. Modification of the traditional LbL-coating technique using a washless protocol allowed the use of smaller amounts of PE, avoiding excessive washed out PEs. Less material was used, and often complicated procedures with centrifugations, filtrations, and intermediate PE washings were avoided, allowing for the process scale-up.

With this we changed a traditional LbL microencapsulation approach for well-soluble drugs encased in polyelectrolyte multilayer shells which slowed down dissolution, to a nanoarchitectural design of well-dispersed low solubility drug nanocolloids stabilized with strongly charged polyelectrolyte shells.

LbL NPs presented important characteristics necessary for improved drug delivery related to nanotechnology. The attainment of a tunable PE LbL multilayer shell offered structural control over the size and surface charge, high encapsulation efficiency, controlled drug release, and absence of in vitro toxicity. This technique also has been shown to be a simple coating technique at the nanoscale, without the use of any special equipment, harsh chemicals, or extreme temperature. It does not require stabilizers, and the medium is water, absent the use of organic solvents.

Thus, LbL nanocoating technology offers promising scaling-up perspectives in obtaining an effective delivery system for low aqueous soluble drugs. For effective oral drug delivery, further work is being developed in order to optimize controlled drug release.

ASSOCIATED CONTENT

Supporting Information

Statistical analysis and microscopic analysis results of LbL NPs, namely, SEM and confocal fluorescent images. The Supporting Information is available free of charge on the ACS Publications website at DOI: 10.1021/acsami.5b02002.

AUTHOR INFORMATION

Corresponding Author

*E-mail: aribeiro@ff.uc.pt. Phone: +351 239 488 400. Fax: +351-239488503.

Notes

The authors declare no competing financial interest.

ACKNOWLEDGMENTS

The authors greatly acknowledge the gift of ibuprofen from Medinfar. The authors wish to thank Dr. Olga Borges from Center for Neuroscience and Cell Biology and Faculty of Pharmacy of University of Coimbra for her kind support with cytotoxicity assays. They are grateful to Dr. Luísa Cortes from the Imaging facility of Center for Neuroscience and Cell Biology for the image acquisition and image analysis. The authors would also like to thank Dr. João Casalta-Lopes for support in the performance of statistical analysis.

ABBREVIATIONS

LbL, layer-by-layer
PAH, poly(allylamine hydrochloride)
PSS, polystyrenesulfonate
NP, nanoparticle
PE, polyelectrolyte
BCS, biopharmaceutics blassification system
PDDA, poly(diallyldimethylammonium chloride)
BSA, bovine serum albumin
GI, gastrointestinal
IBF, ibuprofen
FITC, fluorescein isothiocyanate
MTT, 3-(4,5-dimethylthiazol-2-yl)-2,5-diphenyltetrazolium bromide
DMEM, Dulbecco's modified Eagle's medium
FBS, fetal bovine serum
PDI, polydispersity index
DLS, dynamic light scaterring
ELS, electrophoretic light scattering
SEM, scanning electron microscopy
DMSO, dimethyl sulfoxide
EE, encapsulation efficiency
HPLC, high performance liquid chromatography
UV, ultraviolet

DOI: 10.1021/acsami.5b02002
ACS Appl. Mater. Interfaces 2015, 7, 11972−11983

USP, United States Pharmacopeia
IC_{50}, half maximal inhibitory concentration

REFERENCES

(1) Kesisoglou, F.; Panmai, S.; Wu, Y. Nanosizing—Oral Formulation Development and Biopharmaceutical Evaluation. *Adv. Drug Delivery Rev.* **2007**, *59*, 631−644.
(2) Szczepanowicz, K.; Hoel, H. J.; Szyk-Warszynska, L.; Bielańska, E.; Bouzga, A. M.; Gaudernack, G.; Simon, C.; Warszynski, P. Formation of Biocompatible Nanocapsules with Emulsion Core and Pegylated Shell by Polyelectrolyte Multilayer Adsorption. *Langmuir* **2010**, *26*, 12592−12597.
(3) Torchilin, V. P. Multifunctional Nanocarriers. *Adv. Drug Delivery Rev.* **2006**, *58*, 1532−1555.
(4) Shutava, T. G.; Balkundi, S. S.; Vangala, P.; Steffan, J. J.; Bigelow, R. L.; Cardelli, J. A.; O'Neal, D. P.; Lvov, Y. M. Layer-by-Layer-Coated Gelatin Nanoparticles as a Vehicle for Delivery of Natural Polyphenols. *ACS Nano* **2009**, *3*, 1877−1885.
(5) Zhang, L.; Gu, F. X.; Chan, J. M.; Wang, A. Z.; Langer, R. S.; Farokhzad, O. C. Nanoparticles in Medicine: Therapeutic Applications and Developments. *Clin. Pharmacol. Ther. (N.Y., NY, U.S.)* **2008**, *83*, 761−769.
(6) Yan, Y.; Björnmalm, M.; Caruso, F. Assembly of Layer-by-Layer Particles and Their Interactions with Biological Systems. *Chem. Mater.* **2014**, *26*, 452−460.
(7) Wang, Y.; Hosta-Rigau, L.; Lomas, H.; Caruso, F. Nanostructured Polymer Assemblies Formed at Interfaces: Applications from Immobilization and Encapsulation to Stimuli-Responsive Release. *Phys. Chem. Chem. Phys.* **2011**, *13*, 4782−4801.
(8) Agarwal, A.; Lvov, Y.; Sawant, R.; Torchilin, V. Stable Nanocolloids of Poorly Soluble Drugs with High Drug Content Prepared Using the Combination of Sonication and Layer-by-Layer Technology. *J. Controlled Release* **2008**, *128*, 255−260.
(9) Balabushevich, N. G.; Izumrudov, V. A.; Larionova, N. I. Protein Microparticles with Controlled Stability Prepared Via Layer-by-Layer Adsorption of Biopolyelectrolytes. *Polym. Sci., Ser. A* **2012**, *54*, 540−551.
(10) De Villiers, M. M.; Lvov, Y. M. Layer-by-Layer Self-Assembled Nanoshells for Drug Delivery. *Adv. Drug Delivery Rev.* **2011**, *63*, 699−700.
(11) Nokhodchi, A.; Amire, O.; Jelvehgari, M. Physico-Mechanical and Dissolution Behaviours of Ibuprofen Crystals Crystallized in the Presence of Various Additives. *Daru, J. Pharm. Sci.* **2010**, *18*, 74−83.
(12) Hammond, P. T. Polyelectrolyte Multilayered Nanoparticles: Using Nanolayers for Controlled and Targeted Systemic Release. *Nanomedicine (London, U.K.)* **2012**, *7*, 619−622.
(13) Junyaprasert, V. B.; Morakul, B. Nanocrystals for Enhancement of Oral Bioavailability of Poorly Water-Soluble Drugs. *Asian J. Pharm. Sci. (Hong Kong, China)* **2015**, *10*, 13−23.
(14) Pattekari, P.; Zheng, Z.; Zhang, X.; Levchenko, T.; Torchilin, V.; Lvov, Y. Top-Down and Bottom-up Approaches in Production of Aqueous Nanocolloids of Low Solubility Drug Paclitaxel. *Phys. Chem. Chem. Phys.* **2011**, *13*, 9014−9019.
(15) Shutava, T. G.; Pattekari, P. P.; Arapov, K. A.; Torchilin, V. P.; Lvov, Y. M. Architectural Layer-by-Layer Assembly of Drug Nanocapsules with Pegylated Polyelectrolytes. *Soft Matter* **2012**, *8*, 9418−9427.
(16) Qiu, X.; Leporatti, S.; Donath, E.; Möhwald, H. Studies on the Drug Release Properties of Polysaccharide Multilayers Encapsulated Ibuprofen Microparticles. *Langmuir* **2001**, *17*, 5375−5380.
(17) De Geest, B. G.; Sukhorukov, G. B.; Mohwald, H. The Pros and Cons of Polyelectrolyte Capsules in Drug Delivery. *Expert Opin. Drug Delivery* **2009**, *6*, 613−624.
(18) Trau, D.; Renneberg, R. Encapsulation of Glucose Oxidase Microparticles within a Nanoscale Layer-by-Layer Film: Immobilization and Biosensor Applications. *Biosens. Bioelectron.* **2003**, *18*, 1491−1499.
(19) De Geest, B. G.; Sanders, N. N.; Sukhorukov, G. B.; Demeester, J.; De Smedt, S. C. Release Mechanisms for Polyelectrolyte Capsules. *Chem. Soc. Rev.* **2007**, *36*, 636−649.
(20) Torchilin, V. P. Multifunctional Pharmaceutical Nanocarriers: Promises and Problems. In *Nanotechnologies for the Life Sciences—Polymeric Nanomaterials (Online)*; Kummar, C. S. S. R., Ed; Nanomaterials for the Life Sciences Series; Wiley-VCH Verlag GmbH & Co. KGaA: Weinheim, Germany, 2012; Vol. *10*, Chapter 5, pp 121−155.
(21) Zheng, Z.; Zhang, X.; Carbo, D.; Clark, C.; Nathan, C.; Lvov, Y. Sonication-Assisted Synthesis of Polyelectrolyte-Coated Curcumin Nanoparticles. *Langmuir* **2010**, *26*, 7679−7681.
(22) Lvov, Y. M.; Pattekari, P.; Zhang, X.; Torchilin, V. Converting Poorly Soluble Materials into Stable Aqueous Nanocolloids. *Langmuir* **2010**, *27*, 1212−1217.
(23) Parekh, G.; Pattekari, P.; Joshi, C.; Shutava, T.; DeCoster, M.; Levchenko, T.; Torchilin, V.; Lvov, Y. Layer-by-Layer Nanoencapsulation of Camptothecin with Improved Activity. *Int. J. Pharm. (Amsterdam, Neth.)* **2014**, *465*, 218−227.
(24) *ISO13321 Methods for Determination of Particle Size Distribution Part 8: Photon Correlation Spectroscopy*; International Organisation for Standardisaton (ISO), 1996.
(25) *ISO22412 Particle Size Analysis—Dynamic Light Scattering*; International Organisation for Standardisation (ISO), 2008.
(26) Hiller, S.; Leporatti, S.; Schnackel, A.; Typlt, E.; Donath, E. Protamine Assembled in Multilayers on Colloidal Particles Can Be Exchanged and Released. *Biomacromolecules* **2004**, *5*, 1580−1587.
(27) Fernandez-Carballido, A.; Herrero-Vanrell, R.; Molina-Martinez, I. T.; Pastoriza, P. Biodegradable Ibuprofen-Loaded Plga Microspheres for Intraarticular Administration. Effect of Labrafil Addition on Release in Vitro. *Int. J. Pharm. (Amsterdam, Neth.)* **2004**, *279*, 33−41.
(28) Tsai, Y. M.; Jan, W. C.; Chien, C. F.; Lee, W. C.; Lin, L. C.; Tsai, T. H. Optimised Nano-Formulation on the Bioavailability of Hydrophobic Polyphenol, Curcumin, in Freely-Moving Rats. *Food Chem.* **2011**, *127*, 918−925.
(29) Bantchev, G.; Lu, Z.; Lvov, Y. Layer-by-Layer Nanoshell Assembly on Colloids through Simplified Washless Process. *J. Nanosci. Nanotechnol.* **2009**, *9*, 396−403.
(30) Losche, M.; Schmitt, J.; Decher, G.; Bouwman, W. G.; Kjaer, K. Detailed Structure of Molecularly Thin Polyelectrolyte Multilayer Films on Solid Substrates as Revealed by Neutron Reflectometry. *Macromolecules (Washington, DC, U.S.)* **1998**, *31*, 8893−8906.
(31) Diez-Pascual, A. M.; Wong, J. E. Effect of Layer-by-Layer Confinement of Polypeptides and Polysaccharides onto Thermoresponsive Microgels: A Comparative Study. *J. Colloid Interface Sci.* **2010**, *347*, 79−89.
(32) Jachimska, B.; Jasiński, T.; Warszyński, P.; Adamczyk, Z. Conformations of Poly(Allylamine Hydrochloride) in Electrolyte Solutions: Experimental Measurements and Theoretical Modeling. *Colloids Surf., A* **2010**, *355*, 7−15.
(33) Strydom, S. J.; Otto, D. P.; Stieger, N.; Aucamp, M. E.; Liebenberg, W.; de Villiers, M. M. Self-Assembled Macromolecular Nanocoatings to Stabilize and Control Drug Release from Nanoparticles. *Powder Technol.* **2014**, *256*, 470−476.
(34) Masum, A. M.; Sharmin, F.; Ashraful, I. S. M.; Reza, S. Enhancement of Solubility and Dissolution Characteristics of Ibuprofen by Solid Dispersion Technique. *Dhaka Univ. J. Pharm. Sci.* **2012**, *11*, 1−6.
(35) Antipov, A. A.; Sukhorukov, G. B.; Leporatti, S.; Radtchenko, I. L.; Donath, E.; Möhwald, H. Polyelectrolyte Multilayer Capsule Permeability Control. *Colloids Surf., A* **2002**, *198*, 535−541.
(36) Fu, Y.; Kao, W. J. Drug Release Kinetics and Transport Mechanisms of Non-Degradable and Degradable Polymeric Delivery Systems. *Expert Opin. Drug Delivery* **2010**, *7*, 429−444.
(37) Patil, P.; Paradkar, A. Porous Polystyrene Beads as Carriers for Self-Emulsifying System Containing Loratadine. *AAPS PharmSciTech* **2006**, *7*, E199−E205.
(38) Civan, F. Scale Effect on Porosity and Permeability: Kinetics, Model, and Correlation. *AIChE J.* **2001**, *47*, 271−287.

DOI: 10.1021/acsami.5b02002
ACS Appl. Mater. Interfaces 2015, 7, 11972−11983

(39) Teo, W. E.; Kaur, S.; Ramakrishna, S. Electrospun Polymer Nanocomposite Fibers: Fabrication and Physical Properties. In *Physical Properties and Applications of Polymer Nanocomposites*; Tjong, S. C., Mai, Y. W., Eds; Woodhead Publishing Series in Composites Science and Engineering; Woodhead Publishing: Cambridge, U.K., 2010; Chapter 18, pp 616−637.
(40) Junghanns, J. U.; Muller, R. H. Nanocrystal Technology, Drug Delivery and Clinical Applications. *Int. J. Nanomed.* **2008**, *3*, 295−309.
(41) Schneider, G.; Decher, G. From Functional Core/Shell Nanoparticles Prepared Via Layer-by-Layer Deposition to Empty Nanospheres. *Nano Lett.* **2004**, *4*, 1833−1839.
(42) Al-Qubaisi, M. S.; Rasedee, A.; Flaifel, M. H.; Ahmad, S. H.; Hussein-Al-Ali, S.; Hussein, M. Z.; Eid, E. E.; Zainal, Z.; Saeed, M.; Ilowefah, M.; Fakurazi, S.; Mohd Isa, N.; El Zowalaty, M. E. Cytotoxicity of Nickel Zinc Ferrite Nanoparticles on Cancer Cells of Epithelial Origin. *Int. J. Nanomed.* **2013**, *8*, 2497−2508.
(43) Gerlier, D.; Thomasset, N. Use of MTT Colorimetric Assay to Measure Cell Activation. *J. Immunol. Methods* **1986**, *94*, 57−63.
(44) Kharlampieva, E.; Kozlovskaya, V. Cytocompatibility and Toxicity of Functional Coatings Engineered at Cell Surfaces. In *Cell Surface Engineering: Fabrication of Functional Nanoshells*; Fakhrullin, R., Choi, I., Lvov, Y., Eds.; The Royal Society of Chemistry: Cambridge, U.K., 2014; Chapter 6, pp 98−125.
(45) Wattendorf, U.; Kreft, O.; Textor, M.; Sukhorukov, G. B.; Merkle, H. P. Stable Stealth Function for Hollow Polyelectrolyte Microcapsules through a Poly(Ethylene Glycol) Grafted Polyelectrolyte Adlayer. *Biomacromolecules* **2008**, *9*, 100−108.
(46) Lewinski, N.; Colvin, V.; Drezek, R. Cytotoxicity of Nanoparticles. *Small* **2008**, *4*, 26−49.
(47) Luo, R.; Neu, B.; Venkatraman, S. S. Surface Functionalization of Nanoparticles to Control Cell Interactions and Drug Release. *Small* **2012**, *8*, 2585−2594.
(48) Horie, M.; Nishio, K.; Kato, H.; Shinohara, N.; Nakamura, A.; Fujita, K.; Kinugasa, S.; Endoh, S.; Yamamoto, K.; Yamamoto, O.; Niki, E.; Yoshida, Y.; Iwahashi, H. In Vitro Evaluation of Cellular Responses Induced by Stable Fullerene C60 Medium Dispersion. *J. Biochem.* **2010**, *148*, 289−298.
(49) Goodman, C. M.; McCusker, C. D.; Yilmaz, T.; Rotello, V. M. Toxicity of Gold Nanoparticles Functionalized with Cationic and Anionic Side Chains. *Bioconjugate Chem.* **2004**, *15*, 897−900.
(50) Veerabadran, N. G.; Price, R. R.; Lvov, Y. M. Clay Nanotubes for Encapsulation and Sustained Release of Drugs. *Nano* **2007**, *02*, 115−120.

DOI: 10.1021/acsami.5b02002
ACS Appl. Mater. Interfaces 2015, 7, 11972−11983